Dexmedetomidine Reduces Propofol-Induced Hippocampal Neuron Injury by Modulating the miR-377-5p/Arc Pathway

Zong Chen
First Affiliated Hospital of Guangdong Pharmaceutical University
Yong Ding
First Affiliated Hospital of Guangdong Pharmaceutical University
Ying Zeng
Shenzhen Shajin Hospital Affiliated to Guangzhou Medical University
Xue-Ping Zhang
ShenZhen People's Hospital
Jian-Yan Chen (chenjianyan@yahoo.com)
First Affiliated Hospital of Guangdong Pharmaceutical University

Research Article

Keywords: Dexmedetomidine, propofol, DNMT3A, methylation, neuroprotection, neurotoxicity, apoptosis, viability

Posted Date: September 22nd, 2021

DOI: https://doi.org/10.21203/rs.3.rs-841956/v1

Version of Record: A version of this preprint was published at BMC Pharmacology and Toxicology on March 25th, 2022. See the published version at https://doi.org/10.1186/s40360-022-00555-9.

Abstract

Background

Propofol and dexmedetomidine (DEX) are widely used in general anesthesia, and exert toxic and protective effects on hippocampal neurons, respectively. The study sought to investigate the molecular mechanisms of DEX-mediated neuroprotection against propofol-induced hippocampal neuron injury in mouse brains.

Methods

Hippocampal neurons of mice were treated with propofol, DEX, and propofol+DEX in *vitro* and in *vivo*. Neuronal apoptosis was evaluated by a means of TUNEL (terminal deoxynucleotidyl transferase dUTP nick end labeling) or Hochest 33258 staining; Arc positive expression in hippocampus tissues was detected using a microscope in immunohistochemistry assays; miRNA-377-5p expression levels were quantified by RT-PCR; the protein levels of Arc, DNMT3A, and DNMT3B were determined using western blot; CCK-8 kit was used to evaluated neuron viability; methylation analysis in miR-377-5p promoter was performed through the methylated DNA immunoprecipitation (MeDIP) assay; luciferase reporter assay was performed to confirm whether Arc was under targeted regulation of miR-377-5p.

Results

In the current study, both *in vitro* and *in vivo*, propofol treatment induced hippocampal neuron apoptosis and suppressed cell viability. DNMT3A and DNMT3B expression levels were decreased following propofol treatment, resulting in lowered methylation in the miR-377-5p promoter region and then enhanced expression of miR-377-5p, leading to a decrease in the expression level of downstream Arc. Conversely, the expression levels of DNMT3A and DNMT3B were increased following DEX treatment, thus methylation in miR-377-5p promoter region was improved, and miR-377-5p expression levels were decreased, leading to an increase in the expression level of downstream Arc. Finally, DEX pretreatment protected hippocampal neurons against propofol-induced neurotoxicity by recover the expression levels of DNMT3A, miR-377-5p, and Arc to the normal levels.

Conclusions

DEX reduced propofol-induced hippocampal neuron injury via the miR-377-5p/Arc signaling pathway.

1. Background

The brain is an organ processing and storing information from the outside circumstances, and memories refer to the information storage through neuronal synaptic connections in the brain. Investigating the molecular mechanism of memory remains a huge challenge in the modern neuroscience, due to the complexity of brain structures. The “engram” was a hypothetical molecular basis of the memory, and theorized that the memory was encoded by some neuronal ensembles sparsely distributed in neural

circuits [1]. The cellular and molecular mechanisms of the “engram” consisted of synaptic changes and modulation of gene expression [2, 3].

Some genes are involved with memory formation, such as *BDNF* (brain derived neurotrophic factor) [4], *REELIN* [5], N-methyl d-aspartate (NMDA) receptor subunit *NR1* [6], NMDA receptor subunit *NR3B* [7], *PPP3CA* (protein phosphatase 3 catalytic subunit alpha) [8], *METTL3* (methyltransferase like 3) [9], CREB (cAMP responsive element binding) [10], *Arc* (activity-regulated cytoskeletal), *Egr1* (early growth response 1) [11], etc. Among these genes, *Arc* and *Egr1* belong to immediate early genes (IEGs), which have been widely used as direct molecular markers to measure neuronal activity for decades, owing to dynamical change in the expression of IEGs promptly in response to neuronal activity [12–16]. Arc is a synaptic activity-induced effector and directly regulated by Egr1, and contributes to modulate the synaptic plasticity associated with learning and memory processing [17].

Arc is associated with memory-related behaviors, for instance, singing-driven Arc expression changes with the amount of songs produced by juvenile songbirds, rather than circadian rhythm [18]. Previous studies demonstrated that abundant Arc proteins were produced when mouse brains were active or sober [19–23]. For human, *Arc* is critical for regulation of synaptic and neuronal plasticity, including long-term change of synaptic strength (long-term potentiation and depression), synaptic scaling, and long-term memory formation. Furthermore, Arc is implicated in memory consolidation and reconsolidation processes, leading to play a crucial role in learning and long-term memory [24, 25]. Furthermore, *Arc* is associated with some potential memory-related behaviors such as drug addiction, a recent study indicated that *Arc* might contribute to drug addiction due to regulation of drug-taking vulnerability [26–28].

Arc protein expression was reported to be suppressed by several anesthetics such as propofol [29, 30]. *Arc* silence promoted neuronal apoptosis and aggravated neuronal death, leading to exacerbate traumatic brain injury [31]. *Arc* dysregulation was correlated with cognitive disorders such as alzheimer disease (AD), autism [32]. Zeng Q, et al. found that *Arc* knockdown increased hippocampal neuron apoptosis and revoked the beneficial effect of 3'-daidzein sulfonate sodium on cognitive impairment, conversely, Arc overexpression increased hippocampal neuronal density and improved learning and memory impairments caused by chronic cerebral hypoperfusion [33]. Despite low-dose propofol was safe for brain growth spurt, recommended or high-dose propofol promoted hippocampal neuroapoptosis and induced cognitive defects. Thus, reduplicative use of propofol triggered long-term cognitive dysfunction [34]. Whether propofol induces hippocampal neuron injury by decreasing Arc expression is unclear.

Dexmedetomidine (DEX), as a highly selective potent α2-adrenoceptor agonist, has been proved to have the neuroprotective potential, and is widely used in anesthesia and intensive care setting for sedate patients [35–40]. DEX possesses sedative, anxiolytic, sympatholytic, analgesic, and anesthetic properties [41]. Like propofol, DEX is widely used for general anesthesia [42]. Both propofol and DEX, as nonbenzodiazepine agents, are recommended by guidelines to be first-line medications to provide light sedation [43]. Previous studies revealed that compared with propofol alone, the combination of low-dose

DEX and propofol could decrease propofol consumption in patients undergoing sedation for ambulatory colonoscopy or magnetic resonance imaging, without enhanced incidence of side effects [44–48]. Moreover, the combination of DEX and propofol was reported to minimize respiratory depressive effects and lessen surgery-stimulated physiologic stress-response [49–51]. Actually, low-dose DEX was effective to alleviate emergence delirium after intravenous propofol anesthesia during tonsillectomy [52].

In accordance with GSE106799 dataset, the expression levels of both Arc and DNMT3A (DNA methyltransferase 3 alpha) were decreased while the miR-377-5p expression level was increased following propofol exposure. Of note, propofol caused 29.0-fold decrease of Arc expression ($P = 0.00035$), suggesting a dramatic impact on Arc-mediated function. There is a CpG island located at -1500 bp in the promoter region of *miR-377* gene, suggesting that miR-377-5p expression is under regulation of DNA methylation. miR-377-5p was predicted to target the 3' untranslated region (3'-UTR) of Arc mRNA, implying that Arc expression is regulated by miR-377-5p. In contrast, our preliminary experiment demonstrated that DEX upregulated the expression of DNMT3A and Arc, but lowered expression of miR-377-5p. Therefore, we hypothesized that DEX reverses the inhibitory effect of propofol on Arc through regulating DNMT3A/miR-377-5p, whereby suppressing the neurotoxicity of propofol. This study focused on identifying this hypothesis.

2. Methods

2.1. Animals and Treatments

All animal experiments performed on live animals were approved by the independent animal ethical committee of the First Affiliated Hospital of Guangdong Pharmaceutical University (Guangdong, China) and adhered to relevant guidelines including the ARRIVE guidelines for animal experiments in the study. C56BL/6 mice (21 ± 3 days) from an inbred colony were provided by the animal department of the Xiangya School of Medicine of Central South University. The mice were randomly divided into four groups: control group (n = 4), propofol group (n = 4.50mg/kg),propofol + DEX group (n = 4.50 mg/kg propofol + 100μg/kg DEX)□DEX group (n = 4, 100μg/kg). All mice were euthanized by decapitation after 4 hours of treatments, and the hippocampi were quickly removed, dissected and frozen in liquid nitrogen. The samples were stored at − 80°C until further study.

2.2. Immunohistochemistry and TUNEL staining

After an overnight baking at 60°C, the thick paraffin sections were deparaffinized, rehydrated, and digested with pepsin. Normal horse or goat serum was used to block non-specific binding sites for 20 minutes. Collagen II or collagen X primary antibodies (Beyotime, Shanghai, China) were added and the slides were incubated at 4°C overnight. On the second day, secondary biotinylated horse or goat anti-mouse antibody was added for 30 minutes, then incubated with streptavidin (TaKaRa, Dalian, China) for 30 minutes. Positive staining was detected by Romulin AEC Chromagen (TaKaRa, Dalian, China). To detect the apoptosis rate of hippocampal neuron after exposure to the study drug, terminal deoxynucleotidyl transferase dUTP nick end labeling (TUNEL) staining was performed using a kit in

accordance with the manufacturer's instructions (Applied Biosystems, Foster City, CA, USA). Hippocampal tissues harvested from mice brains were embedded in OCT compound (Applied Biosystems, Foster City, CA, USA). After snapping frozen at − 80°C, four frozen sections with 8mm thickness on cryostat were collected to one slide. Frozen sections were fixed with 4% paraformaldehyde (Abcam, Cambridge, England, UK) for 15 min. The section was stained first with TUNEL (Beijing Solarbio Science & Technology Co.) in light of the manufacturer's instructions. After washing and blocking, biotinylated anti-MCMV early antigen (EA) (Beijing Solarbio Science & Technology Co.) was incubated in the section at 4°C overnight. Texas Red-labeled avidin (Wetzlar, Hessen, Germany) was then used for binding to Biotin for one hour at 25°C. The slides were then mounted with antifade medium containing DAPI (Beijing Solarbio Science & Technology Co.) and observed by microscope. Or the section was stained with fluorescein isothiocyanate (Wetzlar, Hessen, Germany)-conjugated EA and subsequent RPE65 antibody provided by Beijing Solarbio Science & Technology Co., or glial fibrillary acidic protein (GFAP) antibody (Beijing Solarbio Science & Technology Co.).

2.3. Cell culture and treatments

The HT22 cell line derived from mouse hippocampal neurons was purchased from Beijing Solarbio Science & Technology Co.. Cells were cultured in DMEM (dulbecco's modified eagle medium) medium (Sigma-Aldrich, St Louis,MO, USA) supplemented with 10% fetal bovine serum (Sigma-Aldrich, St Louis,MO, USA). The culture plates were incubated at 37 ℃ in a humidified atmosphere containing 5% CO_2. In order to generate the in vitro propofol injury model as previously described, HT22 cells were equally divided into four groups: control group, propofol group (50 μM), propofol (50 μM) + DEX group (50 μM), DEX group (50 μM). HT22 cells of each group were seeded in six-well tissue culture plates overnight. After administration of the study drug, HT22 cells were seeded at 37 ℃ in a humidified atmosphere of 5% CO_2 for 24 hours. HT22 cells were harvested and fixed in cold 80% ethanol after drug treatment, followed by centrifugation and washing, fixed cells were used for further assays.

2.4. Hoechst 33258 staining

HT22 cells were seeded onto clean and sterile coverslips placing on 6-well plates, with a density of 2×10^5 cells. After exposure to the indicated drug or the control for 24 hours, the HT22 cells were stained with 0.5 mL Hoechst 33258 solution (Beyotime) for 5 min. The morphological changes of HT22 cells involving blue nuclei were observed using fluorescence microscopy (Bioworld Technology, St Louis Park, MN, USA).

2.5. CCK-8 assay and cell growth curves

After corresponding treatment, HT22 cells were suspended and counted using an automated cell counter (Roche Diagnostics). Approximately 3.0×10^3 cells per well were seeded into 96-well plates in triplicate. Then, cell viability was examined using a Cell Counting Kit-8 (CCK-8; Sigma-Aldrich, St Louis,MO, USA) according to the manufacturer's protocol. Briefly, 10 ml of CCK-8 solution was added to each well at the time-points of 0, 12, 24, 48, 72. After 2 h of culture at 37 ℃, the optical density (OD) value was monitored with a plate reader at 450 nm (Sigma-Aldrich, St Louis,MO, USA). The cell growth curves were drawn based on OD values every 24 h.

2.6. Western blot analysis

Proteins from mouse hippocampi were extracted on ice by lysis buffer (Beyotime, Jiangsu, China). Total proteins were isolated from cells lysed with RIPA reagent (Roche Diagnostics,Mannheim, Germany) supplemented with 1 mM phenylmethylsulphonyl fluoride (Sigma-Aldrich, St Louis,MO, USA). Then, the protein concentration was measured using a BCA protein assay kit (Sigma-Aldrich, St Louis,MO, USA). Thereafter, equal quantities of proteins were separated by 10% sodium dodecyl sulphate–polyacrylamide gel electrophoresis (Beyotime, Jiangsu, China) and then transferred to polyvinylidene difluoride membranes (Roche Diagnostics, Mannheim, Germany). After blocking with 5% fat-free milk for 2 h at room temperature, the membranes were incubated with primary antibodies at 4 ℃ overnight, which were summarized in Table 1. The membranes were washed three times for 10 min each time in 1×Tris buffered saline/0.1%. Tween-20 (TBST; pH 7.4) at room temperature. Then, the membranes were incubated with horseradish peroxidase-conjugated goat anti-rabbit immunoglobulin G secondary antibodies (1:4000; Cell Signaling TechnologyVR, Danvers, MA, USA) for 1 h at room temperature. The membranes were washed three times for 10 min each time in 1×TBST (pH 7.4) at room temperature. The proteins were visualized using the ChemiDocTM MP Imaging System (Cell Signaling TechnologyVR, Danvers, MA, USA). Experiments were repeated in triplicate.

Table 1
Primary antibodies used for western blot analyses.

Primary antibodies	MW (kDa)	Dilution	Company	Catalog
DNMT3A	≈ 102	1:500	Abcam, Shanghai, China	ab228691
DNMT3B	≈ 95	1:1000	Ptgcn, Chicago, USA	26971-1-AP
Arc	≈ 45	1:500	Ptgcn, Chicago, USA	16290-1-AP
Caspase-3	≈ 1735	1:2000	Abcam, Shanghai, China	ab228691
β-actin	42	1:2000	Ptgcn, Chicago, USA	66009-1-Ig

2.7. Western blot analysis

Total RNA was isolated from the primary NSCs using TRIzol reagent (ThermoFisher, Waltham, MA, USA) following the manufacturer's protocol and 1 μg of RNA was used to synthesize cDNA with SuperScriptase III (ThermoFisher) using random primers for mRNA analysis. MiRNAs were isolated using RNAiso for small RNA (TaKaRa, Dalian, China) following the manufacturer's protocol and 5 μg of RNA was polyadenylated and used to synthesize cDNA with the MirX miRNA First Strand Synthesis kit (Clontech, Nojihigashi, Japan). Expression of mRNA and miRNA was determined by quantitative realtime PCR (qPCR) using the SYBR Green PCR Kit (Qiagen, Duesseldorf, Germany) and MirX miRNA qRT-PCR SYBR Kit (Clontech, Nojihigashi, Japan), respectively. qPCR was performed on the Stratagene Mx3000P Real-Time PCR System (Agilent, Santa Clara, USA) with the following conditions: denaturation at 95°C for 10 s, followed by 40 cycles of 95°C for 5 s and 60°C for 20 s. Three biological samples were each tested in

triplicate for each sample. All experiments were repeated three times. GAPDH and U6 were used as endogenous controls for mRNA and miRNA analysis, respectively. The primers sequences used in this analysis are shown in Table 2. Changes in relative expression were determined using the second derivative maximum method 2-ΔCT calculated by subtracting the cycle threshold (CT) of the endogenous control gene from the CT of the gene of target. Relative fold-changes were calculated using the 2-ΔΔCT method.

Table 2
Primer sequences of RT-PCR.

Gene	Sequence
Dnmt3A	F: AGAAGCCGCTGTTACCTCTT
Dnmt3A	R: GCTGAAACCCTTTGCACAGA
Arc	F: CTGACTCACAACTGCCACAC
Arc	R: TGAGGAAGCCAGATCGTGTT
Caspase-3	F: TCACAGCCGCAACTCAGAC
Caspase-3	G: GGCAGGTCCTGATGAGGTG
β-actin	F: GTGACGTTGACATCCGTAAAGA
β-actin	G: GCCGGACTCATCGTACTCC
miR-377-5p	F: ACACTCCAGCTGGGAGAGGTTGCCCTTGGT
miR-377-5p	G: CTCAACTGGTGTCGTGGAGTCGGCAATTCAGTTGAGGAATTCAC
U6[a]	F: CTCGCTTCGGCAGCACA
U6[a]	G: AACGCTTCACGAATTTGCGT
miR-377-5p[b]	F: AAAATTTTTTTGGGAGAGTTTTTTC
miR-377-5p[b]	G: TTAATAACCATAACCAAACAACGAT
GAPDH[b]	F: CCTTCCCACCCTGTTCATCT
GAPDH[b]	G: AGTTTAGCTGGCCTGGTGAT

2.8. Western blot analysis

Bioinformatics analysis by Alggen revealed a putative binding sit of miR-377-5p (3'-CTTAAGTGGTTCCCGTTGGAGA-5') on the Arc 3'UTR (the binding sequence is 5'-AGGGCAAC-3'). A wild-type sequence containing the binding sit was established by PCR. In addition, the potential binding sit was mutated in the wild-type sequence to established mutant sequence. The wild-type and mutant sequences were cloned and inserted into luciferase report. The vectors were transfected into HT22 cells

alone or with *Arc* over-expression vector using Lipofectamine 2000 (Qiagen, Duesseldorf, Germany). Cells were harvested at 24 h and the activity of firefly luciferase was normalized to that of renilla luciferase.

2.9. DNA Methylation Analysis

DNA methylation analysis was performed through MeDIP assay previously described by Weber, et al. [53] EpiQuik Hydroxymethylated DNA Immunoprecipitation (hMeDIP) Kit (Epigentek, Wuhan, China) was used for the immunoprecipitation, 4 μg of sonicated denatured DNA was incubated with 10 μg of mouse monoclonal antibody against 5-methylcytosine (Ptgcn, Chicago, USA) in 10 × IP buffer (100 mM Na-Phosphate pH 7.0, 1.4 M NaCl, 0.5% Triton X-100) for 6 h at 4 ◦C. Antibody-bound DNA was collected with 80 μl of Dynabeads with M-280 sheep anti-mouse IgG (Ptgcn, Chicago, USA) for 2.15 h at 4 ◦C on a rotating wheel and washed twice with 1×IP buffer (10 mM Na-Phosphate pH 7.0, 0.14 M NaCl, 0.05% Triton X-100). The beads were resuspended in 250 μl Proteinase K buffer (50 mM Tris pH 8.0, 10 mM EDTA, 0.5% SDS, 70 μg proteinase K) and incubated for 5 h at 50 ℃. DNA was extracted from the HT22 cells and treated with bisulfite by using the EpiTect Bisulfite Kit (Clontech, Nojihigashi, Japan). An amount of 2 mL of bisulfite-treated DNA was used for PCR to amplify the miR-377-5p promoter fragment with primers. The fragment capture was performed using Methylamp Methylated DNA Capture (MeDIP) Kit (Clontech, Nojihigashi, Japan). After purification, PCR products were degenerated for 2 min with the sequencing primer at 80 ℃, followed by pyrosequencing on the PyroMark Q96 instrument (Beijing Solarbio Science & Technology Co.).

For the comparison of DNA methylation of the miR-377-5p promoter region in the DNA fragment isolated from HT22 cells, quantitative real-time PCR was used for verifying the enrichment amount for the promoter region of miR-377-5p in the DNA fraction. qPCR was performed with the LightCycler 480 Real-Time PCR System, and the reaction mix contained 1× SYBR green master mix (Roche, Mannheim, Germany) and 0.5 mM of forward and reverse primers, respectively, in a volume of 10 l. PCR cycling consisted of 95 ◦C for 10 min, 45 cycles of 95 ◦C for 10 s, 60 ◦C for 10 s and 72 ◦C for 20 s, followed by a melting curve analysis. The methylated-specific primer for the promoter region of miR-377-5p was designed by MethPrimer (http://www.urogene.org/methprimer/). The forward primer was sense: 5'-AAAATTTTTTTGGGAGAGTTTTTTC-3', and corresponding primer was sense: 5'-TTAATAACCATAACCAAACAACGAT-3'. PCR was performed in accordance with above-mentioned method.

2.10. DNA Methylation Analysis

Data analysis was performed using SPSS 26.0 software (SPSS, Inc., Chicago, IL, USA). Data for densitometry, number of immunopositive cells and TUNEL assay,the expression of DNA and mRNAs were expressed as means ± standard deviation (SD) reflecting the results of independent experiments. In each case the data were reviewed to see how well they fit the assumptions of the tests. The expression of DNA and mRNAs at each timepoint was assessed using Student's t-test. P values < 0.05 were considered to indicate statistical significance.

3. Results

3.1 Bioinformatics analysis for the effects of propofol on the gene expression profiles according to GSE106799 dataset

Using data from GSE106799 dataset, we performed Gene cluster GO analysis revealed the biological functions of neurons influenced by propofol. The up-regulated genes after propofol treatment are primarily associated to biological functions, such as cell signal, cell proliferation, response to hypoxia and so on (Figure 1A). The down-regulated genes after propofol treatment are related to biological functions, such as feeding behavior, long-term memory, negative regulation of transcriptionand so on (Figure 1B). We found that *Arc* gene located in the following pathways: 0007626~locomotory behavior 0007275~multicellular organism development; 0007616~long-term memory, and *Arc* was downregulated after propofol treatment. *DNMT3A* and *DNMT3B* located in the pathway: 0000122~negative regulation of transcription from RNA polymerase II promoter.Treatment with propofol decreased expression of Arc, DNMT3A and DNMT3B (Figure 1C, D & E).

3.2 DEX protects hippocampal neurons from propofol-induced injury in mice with the modulation of miR-377-5p/Arc pathway.

TUNEL staining was performed to identify apoptotic neurons in the mouse hippocampus (Figure 2A). Compared with control group, more TUNEL-stained neurons were observed in the propofol group than those in control group (2.18% ± 0.88% vs 12.45% ± 2.45%, $P = 0.0002$); TUNEL-stained neurons in the propofol+DEX group were decreased significantly compared with propofol group (12.45% ± 2.45% vs 4.78% ± 0.65%, $P = 0.0009$). Immunohistochemistry was performed to evaluate Arc expression in the mouse hippocampus after drug treatment (Figure 2B). Arc positive expression was significantly reduced after propofol treatment compared to the control group (15.95% ± 2.40% vs 5.70% ± 0.80%, $P = 0.002$). Compared with control group, Arc positive expression was elevated following DEX treatment (15.95% ± 2.40% vs 37.08% ± 4.17%, $P = 0.00012$). Moreover, DEX reinstated Arc expression that was down-regulated by propofol (14.38% ± 2.06% vs 37.08% ± 4.17%, $P = 6.5 \times 10^{-5}$).As indicated by RT-PCR,MiR-377-5p expression level was significantly increased after propofol treatment compared to the control group (2.26 ± 0.41 vs 1.18 ± 0.07, $P = 0.043$, Figure 2C). In contrast, MiR-377-5p expression level was significantly decreased after DEX treatment compared to the control group (0.61 ± 0.04 vs 1.18 ± 0.07, $P = 0.0002$). Compared to the control group, MiR-377-5p expression levels in the propofol+DEX group were significantly decreased compared to propofol group (1.27 ± 0.28 vs 2.26 ± 0.41, $P = 0.027$). Western blot analysis showed that propofol significantly decreased DNMT3A, DNMT3B, and Arc proteins in the mouse hippocampus (Figure 2D). After DEX treatment, the protein levels of DNMT3A, DNMT3B, and Arc were all significantly increased compared to the control group. There is no difference in DNMT3A, DNMT3B, and Arc protein levels between propofol+DEX and control groups..

3.3 DEX protects against propofol-induced HT22 cells apoptosis with the modulation of miR-377-5p/Arc pathway.

Using Hoechst 33258 staining, we found cell nucleus shrinkage and chromatin condensation, which are typical apoptotic morphological features, after propofol treatment (Figure 3A). After exposure to propofol, the percent of apoptotic HT22 cells was significantly increased compared with the control group (11.67% ± 1.53% vs 30.33% ± 5.51%, $P = 0.005$Figure 3B). Whereas compared with the propofol group, the propofol+DEX group showed a significantly decrease in the percent of apoptotic HT22 cells (30.33% ± 5.51% vs 16.00% ± 3.00%, $P = 0.017$). There was no significantly difference among the control group, propofol+DEX group, and DEX group in the percent of apoptotic HT22 cells. HT22 cells were exposed to propofol, propofol+DEX, and DEX, followed by analysis of cell viability at 0, 6, 12, 24, 48 h using the CCK-8 assay kit (Figure 3C). After exposure to propofol, HT22 cell viability was significantly inhibited compared to the control group, whereas the introduction of DEX abolished the propofol-induced inhibition. There were no significantly differences among the control group, propofol+DEX group, and DEX groups in the HT22 cell viability. RT-PCR was performed to determine miR-377-5p expression levels in the HT22 cells after exposure to propofol and/or DEX for 24 hours (Figure 3D). MiR-377-5p expression levels in the propofol group were significantly increased compared to the control group, while miR-377-5p expression levels in the propofol+DEX group were significantly decreased compared to the propofol group. After exposure to DEX, miR-377-5p expression levels in the HT22 cells were significantly decreased compared to the control group. Western blot analyses were performed to determine the levels of DNMT3A, DNMT3B, and Arc in HT22 cells (Figure 3E). The results showed exposure to propofol caused significantly decreases in the levels of DNMT3A (Figure 3F), DNMT3B (Figure 3G), and Arc (Figure 3H), while the introduction of DEX counteracted these decreases. The levels of DNMT3A, DNMT3B, and Arc in the propofol+DEX group were all significantly increased compared to the propofol group. After exposure to DEX, the levels of DNMT3A, DNMT3B, and Arc were all significantly increased compared to the control group. DNA methylation in the miR-377-5p promoter was analyzed using MeDIP assay (Figure 3I). The methylation levels in the miR-377-5p promoter were significantly decreased after exposure to propofol, compared to the control group. While compared to the propofol group, the methylation levels of the miR-377-5p were significantly increased in the propofol+DEX group. The methylation levels in the miR-377-5p promoter were significantly increased in the DEX group compared to the control group.

3.4 Arc expression was regulated by DNMT3A/ miR-377-5p pathway

As indicated by RT-PCR, miR-377-5p expression levels were significantly increased in the HT22 cells with DNMT3A knockdown while decreased in the DNMT3A-overexpressed HT22 cells (Figure 4A). Western blot analyses showed that Arc levels were significantly decreased and increased in HT22 cells with DNMT3A knockdown and overexpression, respectively (Figure 4B, 4C, and 4D). To investigate the effect of miR-377-5p on Arc expression, we performed the luciferase report assay to determine interaction between miR-377-5p and Arc mRNA 3'UTR. HT22 cells were co-transfected with luciferase reporter constructs containing wild-type (WT) or mutant-type (MT) Arc 3'UTR and miR-377-5p mimics, and relative luciferase activity was measured and normalized to the negative control (NC) cells (Figure 4E). After transfection of miR-377-5p mimics, the reporter activity of WT Arc construct declined to 47%, while the luciferase activity MT Arc construct was not affected. RT-PCR assay was performed to determine the expression levels of miR-377-5p and Arc after transfection of miR-377-5p mimics and inhibitors. miR-377-5p mimics caused a

significant increase in miR-377-5p expression levels (Figure 4F) and decrease in Arc expression levels compared to the control group (Figure 4G); After transfection with miR-377-5p inhibitor, miR-377-5p expression level was significantly decreased while Arc expression level was significantly increased. Western blot analysis (Figure 4H) showed that Arc levels were decreased and increased after transfection with miR-377-5p mimics and inhibitors (Figure 4I).

3.5 DEX attenuated propofol-induced HT22 cell apoptosis by targeting Arc.

In order to verify that the protective effect of DEX against propofol was associated with *Arc*, we performed *Arc* knockdown alone or in combination with DEX and propofol treatments. Hochest 33258 staining assays were performed to detect the HT22 cell apoptosis after indicated treatments (Figure 5A). DEX suppressed the apoptosis of HT22 cells induced by propofol, however the anti-apoptotic effect of DEX is diminished after Arc knockdown. Silencing Arc independently elevated the percentage of apoptotic cells as well (Figure 5B). CCK-8 assay was performed to analyze HT22 cell viability (Figure 5C). DEX improved HT22 cell viability that was suppressed by propofol. However, this effect of DEX was also abolished with Arc knockdown. Without DEX and propofol treatment, depletion of Arc also decreased HT22 cell viability. RT-PCR analysis showed that propofol decreased DNMT3A but increased miR-377-5p, however these effects of propofol were reversed by DEX independent of Arc knockdown or not (Figure 5D and E). Depletion of Arc diminished the effect of DEX decreasing propofol-induced up-regulation of caspase-3 (Figure 5F). As indicated by western blot assay, propofol decreased DNMT3A and Arc expression, however these effects of propofol were reversed by DEX (Figure 6A, B and C). DNMT3A protein level is not affected by *Arc* knockdown. Propofol induced reduction of pro-caspase-3 but the increase of cleaved caspase-3 (Figure 6 D and E). DEX reversed these actions of propofol, but this effect of DEX was not observed with Arc knockdown.

4. Discussion

Propofol is widely used for general anesthesia especially in intensive care settings [54]. However, propofol-induced cognitive impairment is a prevalent clinical concern [55, 56]. In a rate model, propofol exerted neurotoxicity to the developing brain, because it induced hippocampal neuron apoptosis that contributed to the cognitive impairment [57]. Berndt N, et al. [58] revealed that propofol suppressed complex II of the respiratory chain in CA3 hippocampal area of rat. In the present study, propofol induced hippocampal neuron apoptosis both *in vitro* and *in vivo*, with notably decreases in the expression levels of Arc, DNMT3A, and DNMT3B.

DEX has been identified to attenuate propofol-induced neurotoxicity to hippocampal neurons derived from rats via several signaling pathways, such as Erk1/2/CREB/BDNF, PI3k/Akt/GSK3β, GSK-3β/CRMP2, CDK5/CRMP2, and miR-34a/SIRT1/PI3K/Akt signaling pathways. Previous studies indicated that propofol induced hippocampal neuron injury by elevating apoptosis-related proteins [59–65]. As a protective mechanism, DEX reduced propofol-induced hippocampal neuron injury in rat brains by

increasing miR-34a expression levels. miR-34a decreased SIRT1 expression levels, resulting in activation of the PI3K/Akt pathway [63].

In the present study, we illustrated that propofol treatment caused decreases in DNMT3A and DNMT3B expression levels, which lowered the methylation levels in miR-377-5p promoter region. As a result, miR-377-5p expression was increased, which led to the deficiency of Arc, as it is the target of miR-377-5p. However, DEX treatment enhanced the expression levels of DNMT3A and DNMT3B, thus elevated the methylation levels in the miR-377-5p promoter region, and decreased miR-377-5p expression levels, leading to augment of Arc. Therefore,the addition of DEX attenuated hippocampal neuron injury caused by propofol,

This study found that DNMT3A and DNMT3B played crucial roles in propofol-induced neurotoxicity and DEX-mediated neuroprotection. Actually, DNA methyltransferases (DNMTs) catalyzes DNA methylation and modulates gene expression in central nervous system [66]. DNMTs inhibitor has been reported to have a potential effect on learning involving inhibition of maintenance of long-term potentiation (LTP) associated with learning and impairment of associative learning at hippocampal synapses [67–69]. Changes in hippocampal gene expression of DNMT3A and DNMT3B were correlated with cognitive rehabilitation and neuroprotection in AD [70]. In mature neurons, DNMTs expression was maintained at a high level, and DNMT3A knockout induced the synaptic alteration and learning deficit, which directly influenced learning and memory behavior, thus DNMT3A in the postmitotic neuron was a key regulator in memory formation [71]. DNMT3A loss caused widespread transcriptional alterations and severe impairment of neuronal function [72], and DNMT3A Haploinsufficiency in the brain led to neurodevelopmental disorders involved in growth and behavioral alterations [73]. Recently, it has been revealed that hypoxic preconditioning exerted anti-hypoxic neuroprotection and maintained HT22 cell proliferation and viability through downregulation of the expression levels of DNMT3A and DNMT3B mRNA and protein [74]. Whereas our study illustrated that high expression of DNMT3A was associated with DEX-mediated neuroprotection against hippocampal neuron injury caused by propofol, the results seemed contradictory, maybe due to essential difference between drug treatments and hypoxic preconditioning.

MiR-377-5p was first found by Lucherini OM, et al. [75] that miR-377-5p expression was related to serum amyloid A circulating levels. Afterwards, it was reported that miR-377-5p expression might be implicated in the pathogenesis of latent tuberculosis infection and the recurrence score of breast carcinomas with positive estrogen receptor [76, 77]. Recently, miR-377-5p overexpression was found to inhibit cell development (viability, proliferation, metastasis and invasion) and regulate cell cycle distribution in lung cancers [78, 79]. Moreover, miR-377-5p overexpression aggrandized myocardial dysfunction as well as apoptosis, and promoted the release of inflammatory factors [80]. In contrast, miR-377-5p downregulation suppressed the proliferation and invasion of HepG2 cells belonging to hepatocellular carcinoma cell lines [81]. Taken together, miR-377-5p overexpression was correlated with cell viability and proliferation. Interestingly, Li Y, et al. has demonstrated that miR-377-5p was up-regulated after propofol treatment and contributed to induce neurotoxicity, the result was consistent with our finding [82].

5. Conclusions

This study indicated that propofol induced hippocampal neuron injury characterized by hippocampal neuronal apoptosis and decreased neuronal viability. DEX protected hippocampal neuron against propofol-induced injury by restoring the expression levels of DNMT3A, miR-377-5p, and Arc. Potentially, our findings contribute to provide novel ideas in the development of new drugs for attenuating or eliminating clinical adverse reactions caused by propofol-induced neurotoxicity to hippocampal neurons.

Abbreviations

DEX, dexmedetomidine; TUNEL, terminal deoxynucleotidyl transferase dUTP nick end labeling; methylated DNA immunoprecipitation, MeDIP; BDNF, brain derived neurotrophic factor; NMDA, N-methyl d-aspartate, PPP3CA, protein phosphatase 3 catalytic subunit alpha; METTL3, methyltransferase like 3; CREB, cAMP responsive element binding; Arc, activity-regulated cytoskeletal; Egr1, early growth response 1; IEGs, immediate early genes; AD, alzheimer disease; DNMT3A,DNA methyltransferase 3 alpha;GFAP, glial fibrillary acidic protein; DMEM, dulbecco's modified eagle medium; OD, optical density; SD, standard deviation; DNMTs, DNA methyltransferases; LTP, long-term potentiation; MW, molecule weight; RT-PCR, reverse transcription-polymerase chain reaction; U6, coding gene of U6snRNA; GO, Gene Ontology; MTT, methyl thiazolyl tetrazolium.

Declarations

Ethics approval and consent to participate

All animal experiments performed on live animals were approved by the independent animal ethical committee of the First Affiliated Hospital of Guangdong Pharmaceutical University (Guangdong, China) and adhered to relevant guidelines including the ARRIVE guidelines for animal experiments in the study (NO. GP.62874).

Consent for publication

Not available.

Availability of data and materials

The datasets used and/or analyzed during the current study are available from the corresponding author on reasonable request.

Competing interests

The authors declare that they have no competing interests.

Funding

The work was supported by the Shenzhen Municipal Science and Technology Bureau (project number: JCYJ20170306144452663).

Acknowledgements

We thank the animal department of the Xiangya School of Medicine of Central South University for providing C56BL/6 mice (21 ± 3 days) from an inbred colony. In addition, we thank all members of the laboratory for providing more or less help in our experiments.

Authors' contributions

All authors contributed to the study conception and design. CZ and DY were responsible for performing the experiments and analyzing the experiment results. CZ was responsible for writing the paper, and ZY gave much meaningful guidance advice on the writing. ZXP and CJY were responsible for conducting the experiments and data analyses. CJY was responsible for the submission. All authors reviewed the manuscript and agreed to be accountable for all aspects of the work.

References

1. Tonegawa S, Pignatelli M, Roy DS, Ryan TJ: **Memory engram storage and retrieval**. *Curr Opin Neurobiol* 2015, **35**:101-109.
2. Dudai Y: **Molecular bases of long-term memories: a question of persistence**. *Curr Opin Neurobiol* 2002, **12**(2):211-216.
3. Kandel ER: **The molecular biology of memory storage: a dialogue between genes and synapses**. *Science* 2001, **294**(5544):1030-1038.
4. Geist PA, Dulka BN, Barnes A, Totty M, Datta S: **BNDF heterozygosity is associated with memory deficits and alterations in cortical and hippocampal EEG power**. *Behav Brain Res* 2017, **332**:154-163.
5. Rogers JT, Weeber EJ: **Reelin and apoE actions on signal transduction, synaptic function and memory formation**. *Neuron Glia Biol* 2008, **4**(3):259-270.
6. Wang KW, Ye XL, Huang T, Yang XF, Zou LY: **Optogenetics-induced activation of glutamate receptors improves memory function in mice with Alzheimer's disease**. *Neural Regen Res* 2019, **14**(12):2147-2155.
7. Wang D, Jacobs SA, Tsien JZ: **Targeting the NMDA receptor subunit NR2B for treating or preventing age-related memory decline**. *Expert Opin Ther Targets* 2014, **18**(10):1121-1130.
8. Thapak P, Bishnoi M, Sharma SS: **Pharmacological Inhibition of Transient Receptor Potential Melastatin 2 (TRPM2) Channels Attenuates Diabetes-induced Cognitive Deficits in Rats: A Mechanistic Study**. *Curr Neurovasc Res* 2020, **17**(3):249-258.
9. Zhang Z, Wang M, Xie D, Huang Z, Zhang L, Yang Y, Ma D, Li W, Zhou Q, Yang YG *et al*: **METTL3-mediated N(6)-methyladenosine mRNA modification enhances long-term memory consolidation**. *Cell Res* 2018, **28**(11):1050-1061.

10. Silva AJ, Kogan JH, Frankland PW, Kida S: **CREB and memory**. *Annu Rev Neurosci* 1998, **21**:127-148.
11. Gallo FT, Katche C, Morici JF, Medina JH, Weisstaub NV: **Immediate Early Genes, Memory and Psychiatric Disorders: Focus on c-Fos, Egr1 and Arc**. *Frontiers in Behavioral Neuroscience* 2018, **12**.
12. Link W, Konietzko U, Kauselmann G, Krug M, Schwanke B, Frey U, Kuhl D: **Somatodendritic expression of an immediate early gene is regulated by synaptic activity**. *Proc Natl Acad Sci U S A* 1995, **92**(12):5734-5738.
13. Saffen DW, Cole AJ, Worley PF, Christy BA, Ryder K, Baraban JM: **Convulsant-induced increase in transcription factor messenger RNAs in rat brain**. *Proceedings of the National Academy of Sciences* 1988, **85**(20):7795-7799.
14. Morgan JI, Cohen DR, Hempstead JL, Curran T: **Mapping patterns of c-fos expression in the central nervous system after seizure**. *Science* 1987, **237**(4811):192-197.
15. Zangenehpour S, Chaudhuri A: **Differential induction and decay curves of c-fos and zif268 revealed through dual activity maps**. *Molecular Brain Research* 2002, **109**(1-2):221-225.
16. Bisler S, Schleicher A, Gass P, Stehle JH, Zilles K, Staiger JF: **Expression of c-Fos, ICER, Krox-24 and JunB in the whisker-to-barrel pathway of rats: time course of induction upon whisker stimulation by tactile exploration of an enriched environment**. *Journal of Chemical Neuroanatomy* 2002, **23**(3):187-198.
17. Li L, Carter J, Gao X, Whitehead J, Tourtellotte WG: **The neuroplasticity-associated arc gene is a direct transcriptional target of early growth response (Egr) transcription factors**. *Mol Cell Biol* 2005, **25**(23):10286-10300.
18. Hayase S, Wada K: **Singing activity-driven Arc expression associated with vocal acoustic plasticity in juvenile songbird**. *Eur J Neurosci* 2018, **48**(2):1728-1742.
19. Gao X, Grendel J, Muhia M, Castro-Gomez S, Susens U, Isbrandt D, Kneussel M, Kuhl D, Ohana O: **Disturbed Prefrontal Cortex Activity in the Absence of Schizophrenia-Like Behavioral Dysfunction in Arc/Arg3.1 Deficient Mice**. *J Neurosci* 2019, **39**(41):8149-8163.
20. Honjoh S, de Vivo L, Okuno H, Bito H, Tononi G, Cirelli C: **Higher Arc Nucleus-to-Cytoplasm Ratio during Sleep in the Superficial Layers of the Mouse Cortex**. *Front Neural Circuits* 2017, **11**:60.
21. Penrod RD, Kumar J, Smith LN, McCalley D, Nentwig TB, Hughes BW, Barry GM, Glover K, Taniguchi M, Cowan CW: **Activity-regulated cytoskeleton-associated protein (Arc/Arg3.1) regulates anxiety- and novelty-related behaviors**. *Genes Brain Behav* 2019, **18**(7):e12561.
22. Qiu J, Dunbar DR, Noble J, Cairns C, Carter R, Kelly V, Chapman KE, Seckl JR, Yau JL: **Decreased Npas4 and Arc mRNA Levels in the Hippocampus of Aged Memory-Impaired Wild-Type But Not Memory Preserved 11beta-HSD1 Deficient Mice**. *J Neuroendocrinol* 2016, **28**(1).
23. Suzuki A, Yanagisawa M, Greene RW: **Loss of Arc attenuates the behavioral and molecular responses for sleep homeostasis in mice**. *Proc Natl Acad Sci U S A* 2020, **117**(19):10547-10553.
24. Kedrov AV, Durymanov M, Anokhin KV: **The Arc gene: Retroviral heritage in cognitive functions**. *Neurosci Biobehav Rev* 2019, **99**:275-281.

25. Nikolaienko O, Patil S, Eriksen MS, Bramham CR: **Arc protein: a flexible hub for synaptic plasticity and cognition**. *Semin Cell Dev Biol* 2018, **77**:33-42.
26. Robbins TW, Ersche KD, Everitt BJ: **Drug addiction and the memory systems of the brain**. *Ann N Y Acad Sci* 2008, **1141**:1-21.
27. Hyman SE, Malenka RC, Nestler EJ: **Neural mechanisms of addiction: the role of reward-related learning and memory**. *Annu Rev Neurosci* 2006, **29**:565-598.
28. Penrod RD, Thomsen M, Taniguchi M, Guo Y, Cowan CW, Smith LN: **The activity-regulated cytoskeleton-associated protein, Arc/Arg3.1, influences mouse cocaine self-administration**. *Pharmacol Biochem Behav* 2020, **188**:172818.
29. Whittington RA, Bretteville A, Virag L, Emala CW, Maurin TO, Marcouiller F, Julien C, Petry FR, El-Khoury NB, Morin F *et al*: **Anesthesia-induced hypothermia mediates decreased ARC gene and protein expression through ERK/MAPK inactivation**. *Sci Rep* 2013, **3**:1388.
30. Ren Y, Zhang FJ, Xue QS, Zhao X, Yu BW: **Bilateral inhibition of gamma-aminobutyric acid type A receptor function within the basolateral amygdala blocked propofol-induced amnesia and activity-regulated cytoskeletal protein expression inhibition in the hippocampus**. *Anesthesiology* 2008, **109**(5):775-781.
31. Chen T, Zhu J, Wang Y-H, Hang C-H: **Arc silence aggravates traumatic neuronal injury via mGluR1-mediated ER stress and necroptosis**. *Cell Death & Disease* 2020, **11**(1).
32. Wilkerson JR, Albanesi JP, Huber KM: **Roles for Arc in metabotropic glutamate receptor-dependent LTD and synapse elimination: Implications in health and disease**. *Semin Cell Dev Biol* 2018, **77**:51-62.
33. Zeng Q, Huang Z, Zhang J, Liu R, Li X, Zeng J, Xiao H: **3'-Daidzein Sulfonate Sodium Protects Against Chronic Cerebral Hypoperfusion-Mediated Cognitive Impairment and Hippocampal Damage via Activity-Regulated Cytoskeleton-Associated Protein Upregulation**. *Front Neurosci* 2019, **13**:104.
34. Han D, Jin J, Fang H, Xu G: **Long-term action of propofol on cognitive function and hippocampal neuroapoptosis in neonatal rats**. *Int J Clin Exp Med* 2015, **8**(7):10696-10704.
35. Afonso J, Reis F: **Dexmedetomidine: current role in anesthesia and intensive care**. *Rev Bras Anestesiol* 2012, **62**(1):118-133.
36. Alam A, Suen KC, Hana Z, Sanders RD, Maze M, Ma D: **Neuroprotection and neurotoxicity in the developing brain: an update on the effects of dexmedetomidine and xenon**. *Neurotoxicol Teratol* 2017, **60**:102-116.
37. Peng M, Ling X, Song R, Gao X, Liang Z, Fang F, Cang J: **Upregulation of GLT-1 via PI3K/Akt Pathway Contributes to Neuroprotection Induced by Dexmedetomidine**. *Front Neurol* 2019, **10**:1041.
38. Perez-Zoghbi JF, Zhu W, Grafe MR, Brambrink AM: **Dexmedetomidine-mediated neuroprotection against sevoflurane-induced neurotoxicity extends to several brain regions in neonatal rats**. *Br J Anaesth* 2017, **119**(3):506-516.
39. Sottas CE, Anderson BJ: **Dexmedetomidine: the new all-in-one drug in paediatric anaesthesia?** *Curr Opin Anaesthesiol* 2017, **30**(4):441-451.

40. Wang Y, Han R, Zuo Z: **Dexmedetomidine-induced neuroprotection: is it translational?** *Transl Perioper Pain Med* 2016, **1**(4):15-19.
41. Mahmoud M, Mason KP: **Dexmedetomidine: review, update, and future considerations of paediatric perioperative and periprocedural applications and limitations**. *British Journal of Anaesthesia* 2015, **115**(2):171-182.
42. Davy A, Fessler J, Fischler M, M LEG: **Dexmedetomidine and general anesthesia: a narrative literature review of its major indications for use in adults undergoing non-cardiac surgery**. *Minerva Anestesiol* 2017, **83**(12):1294-1308.
43. Devlin JW, Skrobik Y, Gelinas C, Needham DM, Slooter AJC, Pandharipande PP, Watson PL, Weinhouse GL, Nunnally ME, Rochwerg B *et al*: **Clinical Practice Guidelines for the Prevention and Management of Pain, Agitation/Sedation, Delirium, Immobility, and Sleep Disruption in Adult Patients in the ICU**. *Crit Care Med* 2018, **46**(9):e825-e873.
44. Edokpolo LU, Mastriano DJ, Serafin J, Weedon JC, Siddiqui MT, Dimaculangan DP: **Discharge Readiness after Propofol with or without Dexmedetomidine for Colonoscopy: A Randomized Controlled Trial**. *Anesthesiology* 2019, **131**(2):279-286.
45. Boriosi JP, Eickhoff JC, Klein KB, Hollman GA, Cravero J: **A retrospective comparison of propofol alone to propofol in combination with dexmedetomidine for pediatric 3T MRI sedation**. *Pediatric Anesthesia* 2017, **27**(1):52-59.
46. Han Y, Han L, Dong M, Sun Q, Ding K, Zhang Z, Cao J, Zhang Y: **Comparison of a loading dose of dexmedetomidine combined with propofol or sevoflurane for hemodynamic changes during anesthesia maintenance: a prospective, randomized, double-blind, controlled clinical trial**. *BMC Anesthesiology* 2018, **18**(1).
47. Dutta A, Sethi N, Sood J, Panday BC, Gupta M, Choudhary P, Puri GD: **The Effect of Dexmedetomidine on Propofol Requirements During Anesthesia Administered by Bispectral Index-Guided Closed-Loop Anesthesia Delivery System**. *Anesthesia & Analgesia* 2019, **129**(1):84-91.
48. Nagoshi M, Reddy S, Bell M, Cresencia A, Margolis R, Wetzel R, Ross P: **Low-dose dexmedetomidine as an adjuvant to propofol infusion for children in MRI: A double-cohort study**. *Paediatr Anaesth* 2018, **28**(7):639-646.
49. Ding L, Zhang H, Mi W, Wang T, He Y, Zhang X, Ma X, Li H: **Effects of dexmedetomidine on anesthesia recovery period and postoperative cognitive function of patients after robot-assisted laparoscopic radical cystectomy**. *Int J Clin Exp Med* 2015, **8**(7):11388-11395.
50. Akarsu Ayazoglu T, Polat E, Bolat C, Yasar NF, Duman U, Akbulut S, Yol S: **Comparison of propofol-based sedation regimens administered during colonoscopy**. *Rev Med Chil* 2013, **141**(4):477-485.
51. Candiotti KA, Bergese SD, Bokesch PM, Feldman MA, Wisemandle W, Bekker AY: **Monitored Anesthesia Care with Dexmedetomidine: A Prospective, Randomized, Double-Blind, Multicenter Trial**. *Anesthesia & Analgesia* 2010, **110**(1):47-56.
52. Tsiotou AG, Malisiova A, Kouptsova E, Mavri M, Anagnostopoulou M, Kalliardou E: **Dexmedetomidine for the reduction of emergence delirium in children undergoing tonsillectomy with propofol**

anesthesia: A double-blind, randomized study. *Paediatr Anaesth* 2018, **28**(7):632-638.

53. Weber M, Hellmann I, Stadler MB, Ramos L, Paabo S, Rebhan M, Schubeler D: **Distribution, silencing potential and evolutionary impact of promoter DNA methylation in the human genome**. *Nat Genet* 2007, **39**(4):457-466.
54. Chidambaran V, Costandi A, D'Mello A: **Propofol: a review of its role in pediatric anesthesia and sedation**. *CNS Drugs* 2015, **29**(7):543-563.
55. Rundshagen I: **Postoperative cognitive dysfunction**. *Dtsch Arztebl Int* 2014, **111**(8):119-125.
56. Belrose JC, Noppens RR: **Anesthesiology and cognitive impairment: a narrative review of current clinical literature**. *BMC Anesthesiol* 2019, **19**(1):241.
57. Wang X, Ding G, Lai W, Liu S, Shuai J: **MicroRNA-383 upregulation protects against propofol-induced hippocampal neuron apoptosis and cognitive impairment**. *Exp Ther Med* 2018, **15**(4):3181-3188.
58. Berndt N, Rosner J, Haq RU, Kann O, Kovacs R, Holzhutter HG, Spies C, Liotta A: **Possible neurotoxicity of the anesthetic propofol: evidence for the inhibition of complex II of the respiratory chain in area CA3 of rat hippocampal slices**. *Arch Toxicol* 2018, **92**(10):3191-3205.
59. Lv J, Wei Y, Chen Y, Zhang X, Gong Z, Jiang Y, Gong Q, Zhou L, Wang H, Xie Y: **Dexmedetomidine attenuates propofol-induce neuroapoptosis partly via the activation of the PI3k/Akt/GSK3beta pathway in the hippocampus of neonatal rats**. *Environ Toxicol Pharmacol* 2017, **52**:121-128.
60. Tu Y, Liang Y, Xiao Y, Lv J, Guan R, Xiao F, Xie Y, Xiao Q: **Dexmedetomidine attenuates the neurotoxicity of propofol toward primary hippocampal neurons in vitro via Erk1/2/CREB/BDNF signaling pathways**. *Drug Des Devel Ther* 2019, **13**:695-706.
61. Xiao Y, Zhou L, Tu Y, Li Y, Liang Y, Zhang X, Lv J, Zhong Y, Xie Y: **Dexmedetomidine attenuates the propofol-induced long-term neurotoxicity in the developing brain of rats by enhancing the PI3K/Akt signaling pathway**. *Neuropsychiatr Dis Treat* 2018, **14**:2191-2206.
62. Li J, Guo M, Liu Y, Wu G, Miao L, Zhang J, Zuo Z, Li Y: **Both GSK-3beta/CRMP2 and CDK5/CRMP2 pathways participate in the protection of dexmedetomidine against propofol-induced learning and memory impairment in neonatal rats**. *Toxicol Sci* 2019.
63. Xing N, Xing F, Li Y, Li P, Zhang J, Wang D, Zhang W, Yang J: **Dexmedetomidine improves propofol-induced neuronal injury in rat hippocampus with the involvement of miR-34a and the PI3K/Akt signaling pathway**. *Life Sci* 2020, **247**:117359.
64. Wang Y, Wu C, Han B, Xu F, Mao M, Guo X, Wang J: **Dexmedetomidine attenuates repeated propofol exposure-induced hippocampal apoptosis, PI3K/Akt/Gsk-3beta signaling disruption, and juvenile cognitive deficits in neonatal rats**. *Mol Med Rep* 2016, **14**(1):769-775.
65. Wei Y, Hu J, Liang Y, Zhong Y, He D, Qin Y, Li L, Chen J, Xiao Q, Xie Y: **Dexmedetomidine pretreatment attenuates propofolinduced neurotoxicity in neuronal cultures from the rat hippocampus**. *Mol Med Rep* 2016, **14**(4):3413-3420.
66. Mehler MF: **Epigenetics and the nervous system**. *Ann Neurol* 2008, **64**(6):602-617.

67. Levenson JM, Roth TL, Lubin FD, Miller CA, Huang IC, Desai P, Malone LM, Sweatt JD: **Evidence that DNA (cytosine-5) methyltransferase regulates synaptic plasticity in the hippocampus**. *J Biol Chem* 2006, **281**(23):15763-15773.
68. Miller CA, Campbell SL, Sweatt JD: **DNA methylation and histone acetylation work in concert to regulate memory formation and synaptic plasticity**. *Neurobiol Learn Mem* 2008, **89**(4):599-603.
69. Miller CA, Sweatt JD: **Covalent modification of DNA regulates memory formation**. *Neuron* 2007, **53**(6):857-869.
70. Grinan-Ferre C, Izquierdo V, Otero E, Puigoriol-Illamola D, Corpas R, Sanfeliu C, Ortuno-Sahagun D, Pallas M: **Environmental Enrichment Improves Cognitive Deficits, AD Hallmarks and Epigenetic Alterations Presented in 5xFAD Mouse Model**. *Front Cell Neurosci* 2018, **12**:224.
71. Morris MJ, Adachi M, Na ES, Monteggia LM: **Selective role for DNMT3a in learning and memory**. *Neurobiology of Learning and Memory* 2014, **115**:30-37.
72. Lavery LA, Ure K, Wan YW, Luo C, Trostle AJ, Wang W, Jin H, Lopez J, Lucero J, Durham MA *et al*: **Losing Dnmt3a dependent methylation in inhibitory neurons impairs neural function by a mechanism impacting Rett syndrome**. *Elife* 2020, **9**.
73. Christian DL, Wu DY, Martin JR, Moore JR, Liu YR, Clemens AW, Nettles SA, Kirkland NM, Papouin T, Hill CA *et al*: **DNMT3A Haploinsufficiency Results in Behavioral Deficits and Global Epigenomic Dysregulation Shared across Neurodevelopmental Disorders**. *Cell Rep* 2020, **33**(8):108416.
74. Liu N, Zhang XL, Jiang SY, Shi JH, Cui JH, Liu XL, Han LH, Gong KR, Yan SC, Xie W *et al*: **Neuroprotective mechanisms of DNA methyltransferase in a mouse hippocampal neuronal cell line after hypoxic preconditioning**. *Neural Regen Res* 2020, **15**(12):2362-2368.
75. Lucherini OM, Obici L, Ferracin M, Fulci V, McDermott MF, Merlini G, Muscari I, Magnotti F, Dickie LJ, Galeazzi M *et al*: **First report of circulating microRNAs in tumour necrosis factor receptor-associated periodic syndrome (TRAPS)**. *PLoS One* 2013, **8**(9):e73443.
76. Emmadi R, Canestrari E, Arbieva ZH, Mu W, Dai Y, Frasor J, Wiley E: **Correlative Analysis of miRNA Expression and Oncotype Dx Recurrence Score in Estrogen Receptor Positive Breast Carcinomas**. *PLoS One* 2015, **10**(12):e0145346.
77. Meng QL, Liu F, Yang XY, Liu XM, Zhang X, Zhang C, Zhang ZD: **Identification of latent tuberculosis infection-related microRNAs in human U937 macrophages expressing Mycobacterium tuberculosis Hsp16.3**. *BMC Microbiol* 2014, **14**:37.
78. Wu H, Liu HY, Liu WJ, Shi YL, Bao D: **miR-377-5p inhibits lung cancer cell proliferation, invasion, and cell cycle progression by targeting AKT1 signaling**. *J Cell Biochem* 2018.
79. Tan Z, Cao F, Jia B, Xia L: **Circ_0072088 promotes the development of non-small cell lung cancer via the miR-377-5p/NOVA2 axis**. *Thorac Cancer* 2020, **11**(8):2224-2236.
80. Liang H, Li F, Li H, Wang R, Du M: **Overexpression of lncRNA HULC Attenuates Myocardial Ischemia/reperfusion Injury in Rat Models and Apoptosis of Hypoxia/reoxygenation Cardiomyocytes via Targeting miR-377-5p through NLRP3/Caspase1/IL1beta Signaling Pathway Inhibition**. *Immunol Invest* 2020:1-14.

81. Yan C, Wei S, Han D, Wu L, Tan L, Wang H, Dong Y, Hua J, Yang W: **LncRNA HULC shRNA disinhibits miR-377-5p to suppress the growth and invasion of hepatocellular carcinoma in vitro and hepatocarcinogenesis in vivo**. *Ann Transl Med* 2020, **8**(20):1294.
82. Li Y, Liu Y, Fan J, Zhou Q, Song X, Peng Z, Qin Z, Tao T: **Validation and bioinformatic analysis of propofol-induced differentially expressed microRNAs in primary cultured neural stem cells**. *Gene* 2018, **664**:90-100.

Figures

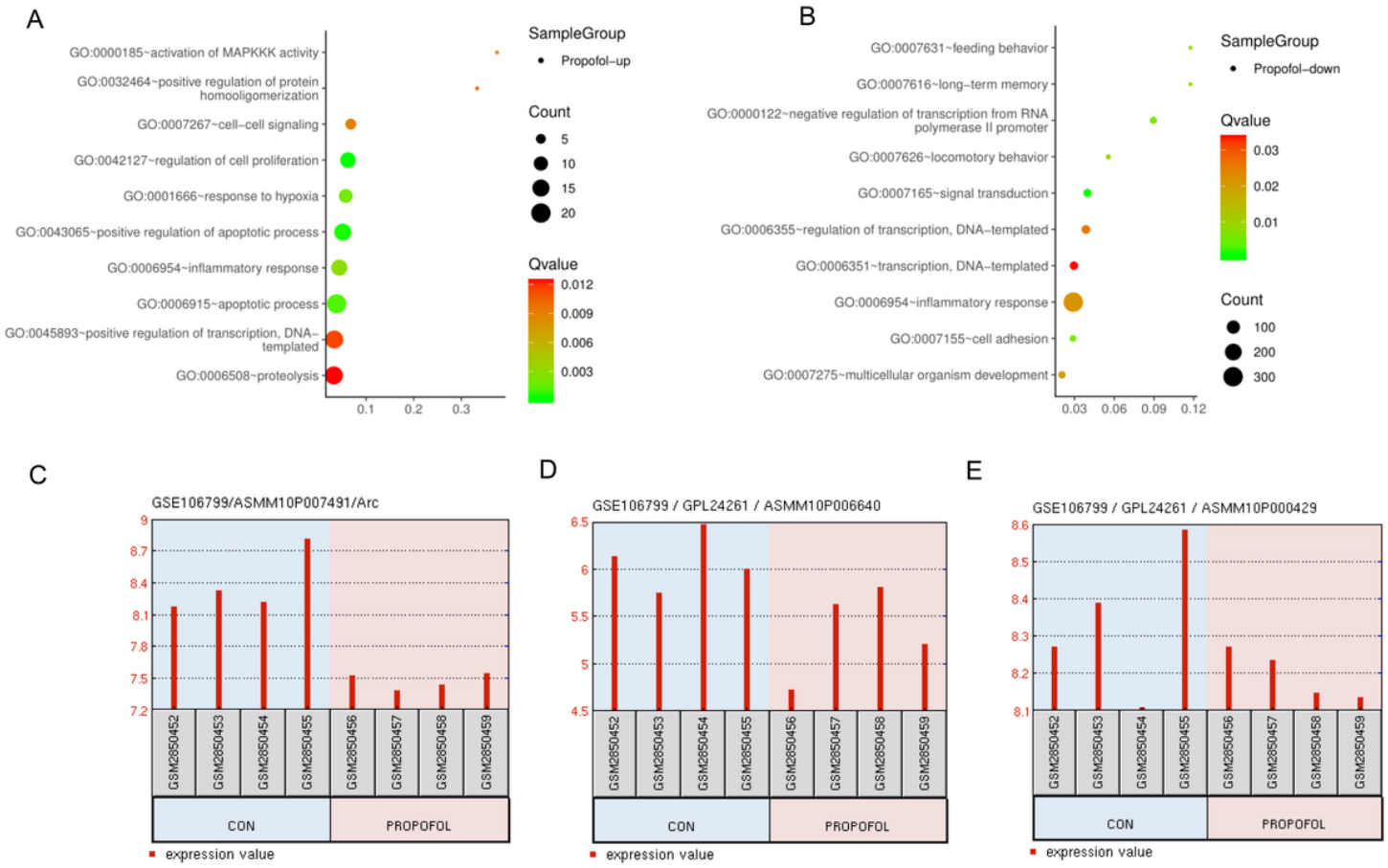

Figure 1

Bioinformatics analysis for effects of propofol on the gene expression profiles according to GSE106799 datasets. Using data from GSE106799 dataset, we performed Gene cluster GO analysis revealed the biological functions of neurons influenced by propofol. A, the up-regulated genes after propofol treatment are primarily associated to biological functions, such as cell signal, cell proliferation, response to hypoxia and so on. B, the down-regulated genes after propofol treatment are related to biological functions, such as feeding behavior, long-term memory, negative regulation of transcription, and so on. Treatment with propofol decreased expression of Arc, DNMT3A and DNMT3B (C, D & E respectively). GO, Gene Ontology,

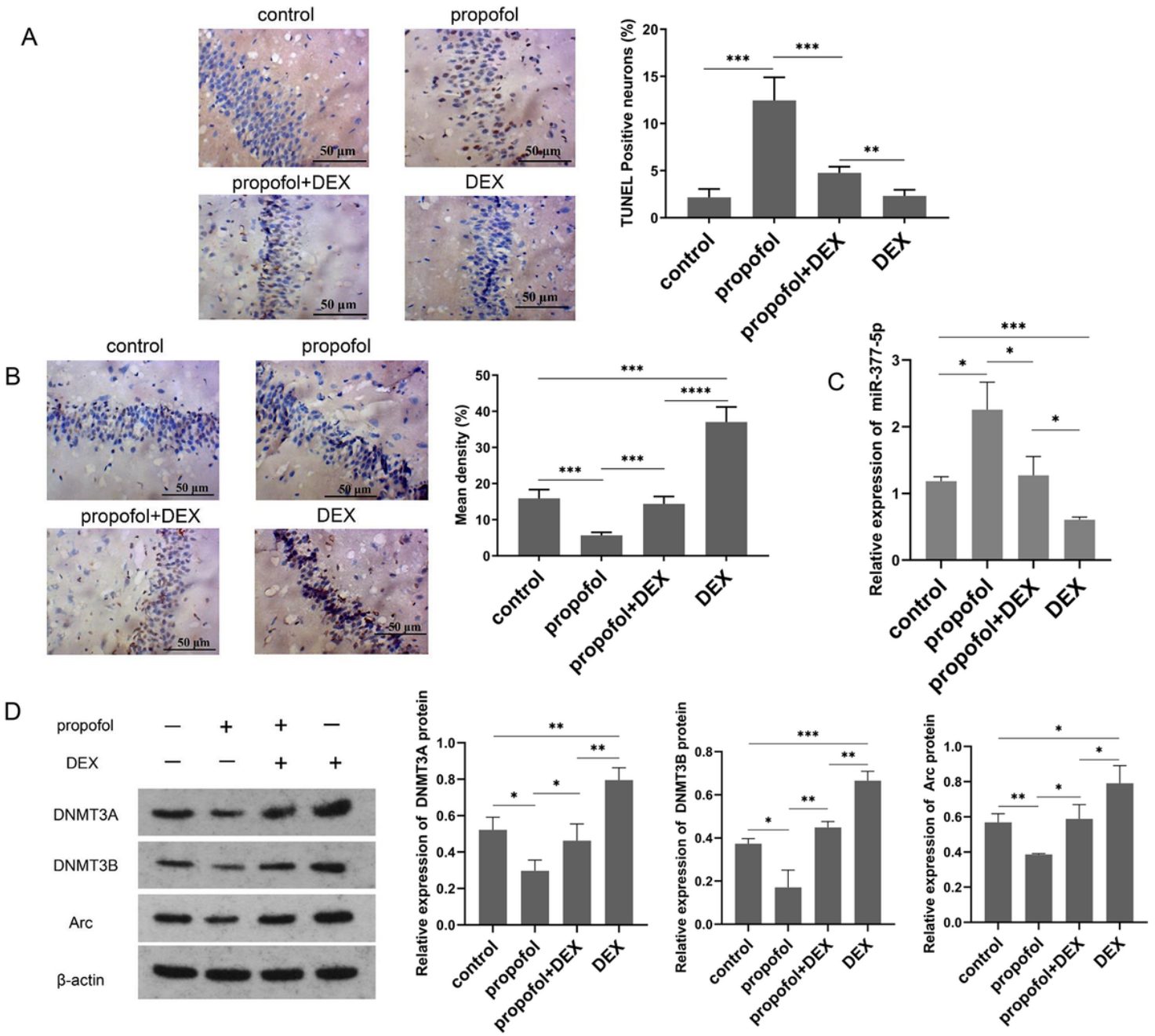

Figure 2

DEX pretreatment reduces the propofol-induced neuronal injury in mouse hippocampus. A, hippocampal neuronal apoptosis in mouse brains measured with TUNEL staining; B, Arc positive expression detected with immunohistochemistry in rat hippocampus; C, miR-377-5p expression levels quantified using PR-PCR; D, protein expression levels of DNMT3A, DNMT3B, and Arc measured using western blot analysis, and the full-length blots/gels are presented in Supplementary Figure S2. Each value represents the mean ± SD for n = 3. *, P < 0.05; **, P < 0.01; ***, P < 0.001. DEX, dexmedetomidine; TUNEL, terminal deoxynucleotidyl transferase (TdT)-mediated dUTP nick end labeling.

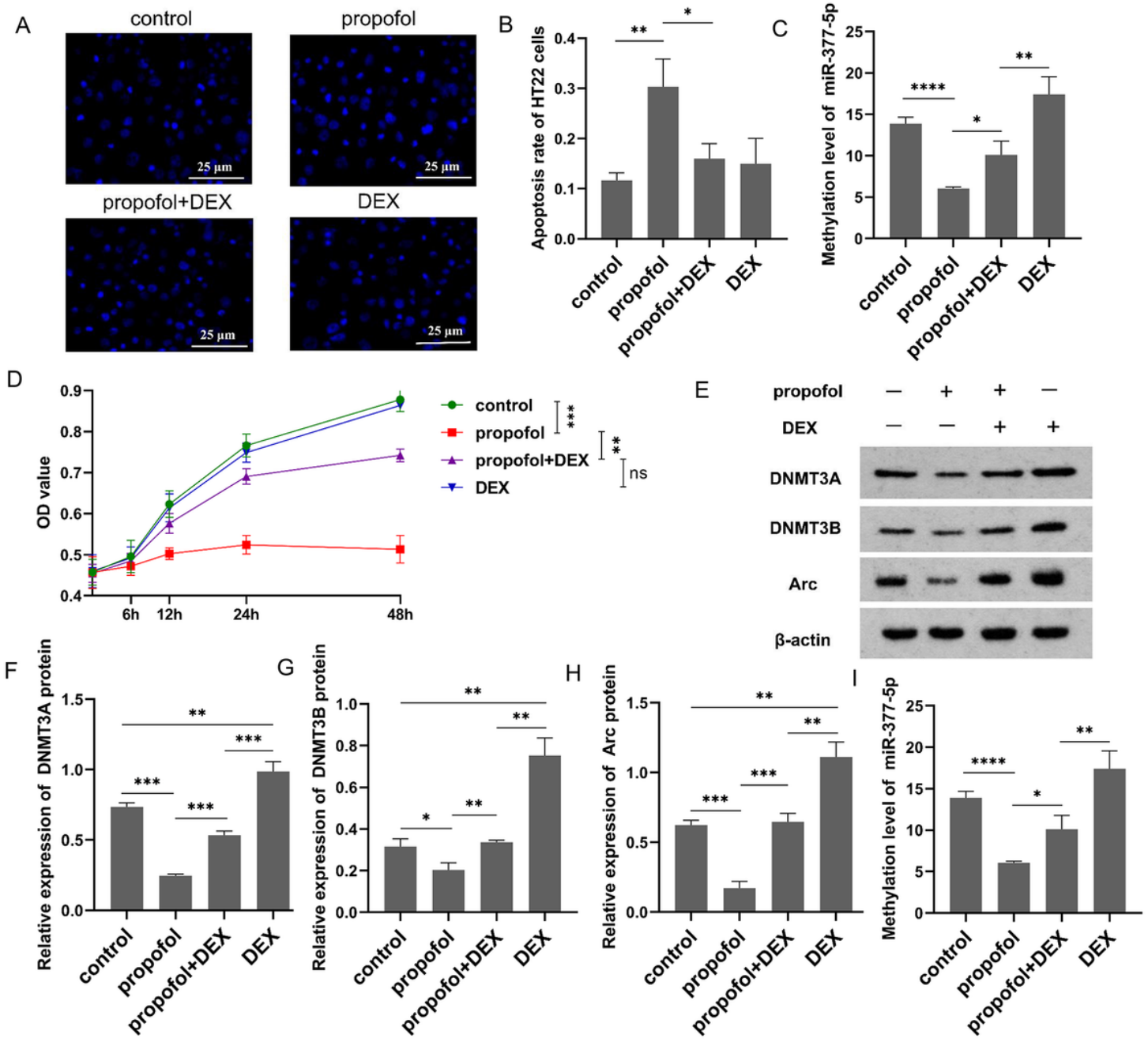

Figure 3

DEX decreases propofol-induced HT22 cell apoptosis via the miR-377-5p/Arc signaling pathway. A, HT22 cell apoptosis detected using Hochest 33258 staining; B, HT22 cell apoptosis rate following exposure to the study drug; C, HT22 cell viability and proliferation determined using MTT kit; D, miR-377-5p expression levels quantified using PR-PCR; E, protein expression levels of DNMT3A (F), DNMT3B (G), and Arc (H) measured using western blot analysis, and the full-length blots/gels are presented in Supplementary Figure S3. I, methylation level in the miR-377-5p promoter region detected through MeDIP assay. Each value represents the mean ± SD for n = 3. *, P < 0.05; **, P < 0.01; ***, P < 0.001; ****, P < 0.0001. DEX, dexmedetomidine; MTT, methyl thiazolyl tetrazolium; MeDIP, methylated DNA immunoprecipitation.

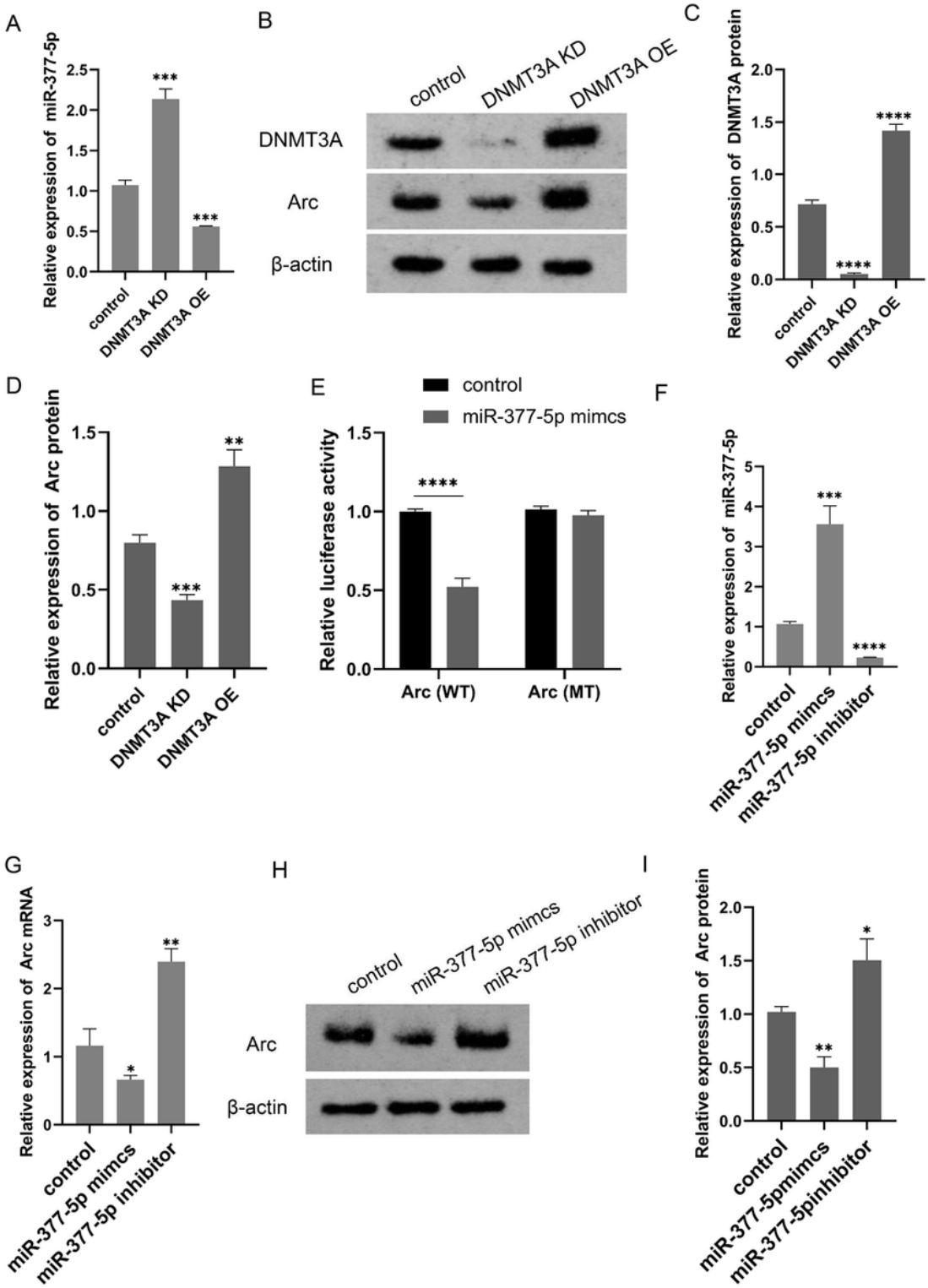

Figure 4

Arc is regulated by DNMT3A/miR-377-5p pathway. A, Arc mRNA expression after DNMT3A knockdown or overexpression quantified using RT-PCR. B, Arc protein expression after DNMT3A knockdown or overexpression identified using western blot analysis, and the full-length blots/gels are presented in Supplementary Figure S4. C, the changes of DNMT3A protein expression after DNMT3A knockdown or overexpression; D, Arc protein expression quantified using western blot analysis. E, targeted regulation of

miR-377-5p on Arc identified through luciferase reporter assay. F, miR-377-5p expression levels after the introduction of miR-377-5p mimcs or inhibitor quantified using PR-PCR; G, Arc mRNA expression levels quantified using RT-PCR; H, the changes of Arc protein expression after the introduction of miR-377-5p mimcs or inhibitor identified using western blot analysis, and the full-length blots/gels are presented in Supplementary Figure S5; I, Arc protein expression levels detected using western blot analysis. Each value represents the mean ± SD for n = 3. *, P < 0.05; **, P < 0.01; ***, P < 0.001; ****, P < 0.0001. DEX, dexmedetomidine.

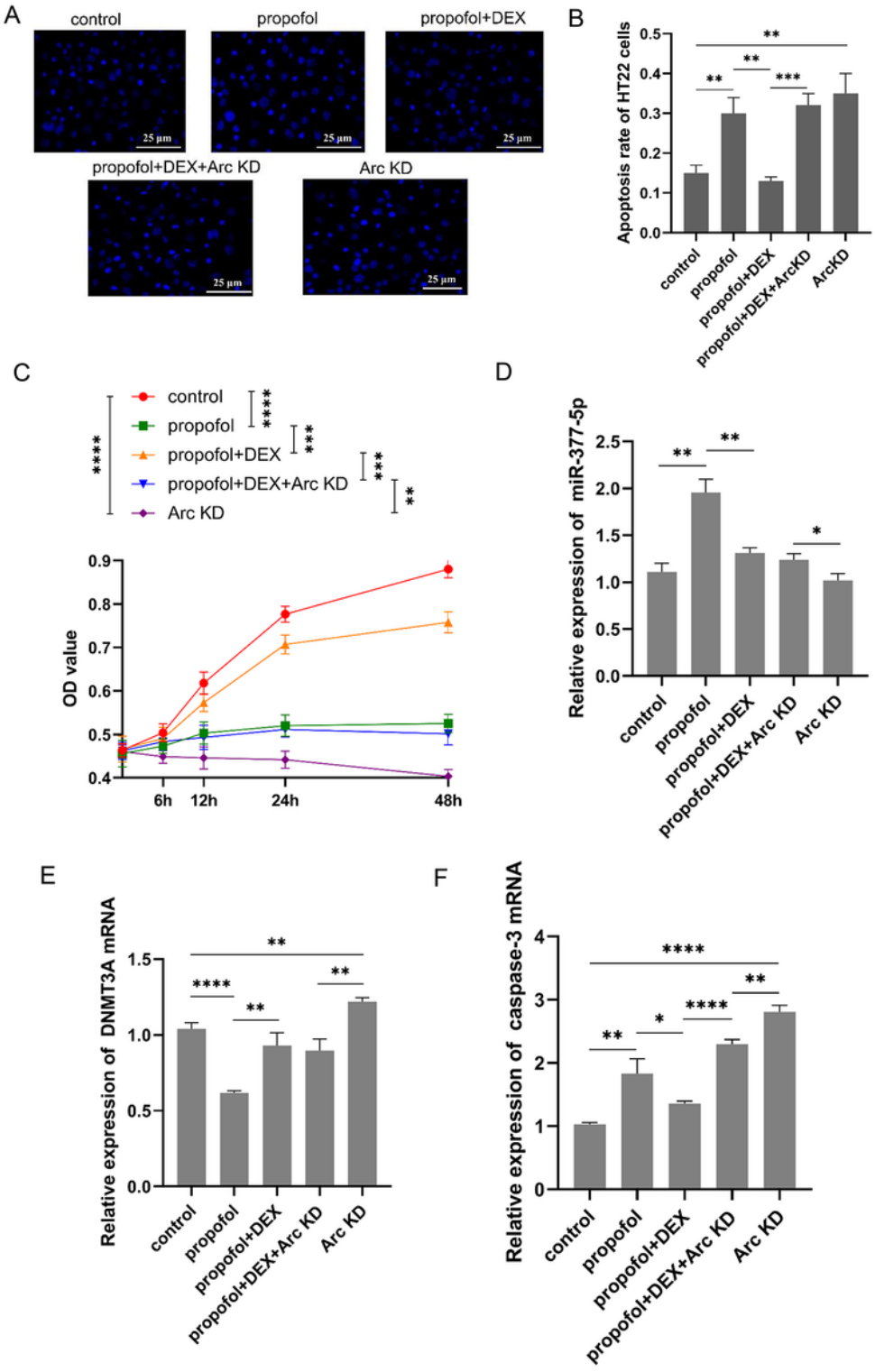

Figure 5

DEX protects HT22 cells against propofol-induced apoptosis by regulating Arc expression. A, HT22 cell apoptosis detected using Hochest 33258 staining; B, HT22 cell apoptosis rate following exposure to the study drug or shArc; C, C, HT22 cell viability and proliferation determined through MTT assay; the mRNA expression levels of miR-377-5p (D), DNMT3A (E), and caspase-3 (F) quantified using RT-PCR. Each value represents the mean ± SD for n = 3. *, P < 0.05; **, P < 0.01; ***, P < 0.001; ****, P < 0.0001. DEX, dexmedetomidine.

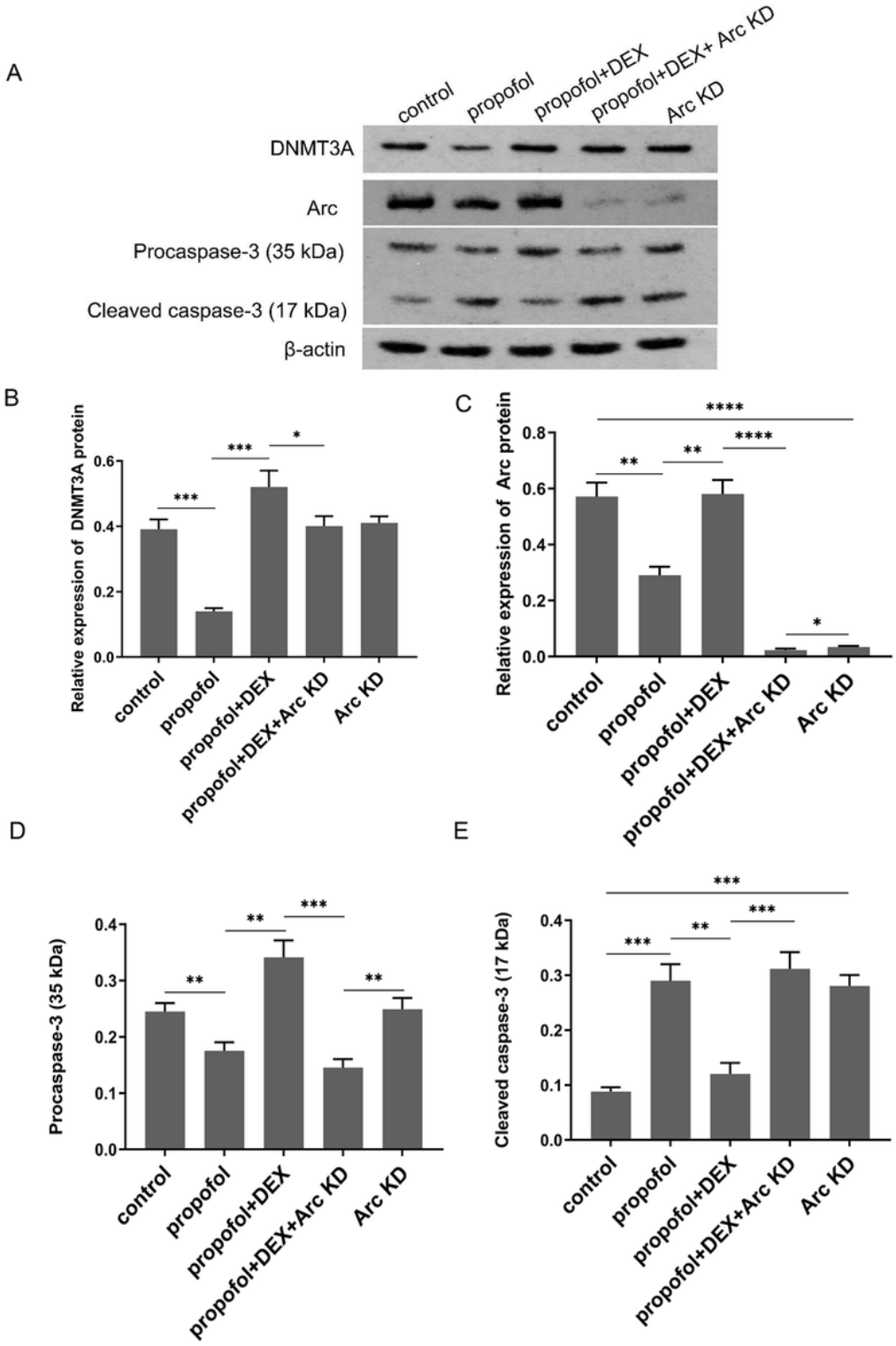

Figure 6

Arc is associated with apoptosis-related protein expression. A, protein expression levels of DNMT3A (B), Arc (C), caspase-3-35 (D), and caspase-3-17 (E) detected using western blot analysis, and the full-length blots/gels are presented in Supplementary Figure S6. Each value represents the mean ± SD for n = 3. *, P < 0.05; **, P < 0.01; ***, P < 0.001; ****, P < 0.0001. DEX, dexmedetomidine.

Supplementary Files

This is a list of supplementary files associated with this preprint. Click to download.

- FigureS1.pdf
- FigureS2.pdf
- FigureS3.pdf
- FigureS4.pdf
- FigureS5.pdf
- FigureS6.pdf